magnetochemistry

MDPI

Article

A Novel Family of Triangular $Co^{II}_2Ln^{III}$ and $Co^{II}_2Y^{III}$ Clusters by the Employment of Di-2-Pyridyl Ketone †

Constantinos G. Efthymiou [1], Áine Ní Fhuaráin [1], Júlia Mayans [2], Anastasios Tasiopoulos [3], Spyros P. Perlepes [4] and Constantina Papatriantafyllopoulou [1,*]

1 SSPC, Synthesis and Solid State Pharmaceutical Centre, School of Chemistry, National University of Ireland Galway, University Road, H91 TK33 Galway, Ireland; dinosef@yahoo.com (C.G.E.); A.NIFHUARAIN1@nuigalway.ie (Á.N.F.)

2 Departament de Quimica Inorgànica i Orgànica, Secció Inorgànica and Institut de Nanociencia I, Nanotecnologia (IN2UB), Universitat de Barcelona, Marti i Franquès 1-11, 08028 Barcelona, Spain; julia.mayans@qi.ub.edu

3 Department of Chemistry, University of Cyprus, 1678 Nicosia, Cyprus; atasio@ucy.ac.cy

4 Department of Chemistry, University of Patras, 26504 Patras, Greece; perlepes@patreas.upatras.gr

* Correspondence: constantina.papatriantafyllopo@nuigalway.ie; Tel.: +353-91-493462

† This paper is dedicated to Professor Masahiro Yamashita, a leading and inspiring Scientist on Molecular Magnetism, on the occasion of his 65th birthday.

Received: 31 March 2019; Accepted: 24 May 2019; Published: 4 June 2019

Abstract: The synthesis, structural characterization and magnetic study of novel Co^{II}/4f and Co^{II}/Y^{III} clusters are described. In particular, the initial employment of di-2-pyridyl ketone, $(py)_2CO$, in mixed metal Co/4f chemistry, provided access to four triangular clusters, $[Co^{II}_2M^{III}\{(py)_2C(OEt)(O)\}_4(NO_3)(H_2O)]_2[M(NO_3)_5](ClO_4)_2$ (M = Gd, **1**; Dy, **2**; Tb, **3**; Y, **4**), where $(py)_2C(OEt)(O)^-$ is the monoanion of the hemiketal form of $(py)_2CO$. Clusters **1**–**4** are the first reported Co/4f (**1**–**3**) and Co/Y (**4**) species bearing $(py)_2CO$ or its derivatives, despite the fact that over 200 metal clusters bearing this ligand have been reported so far. Variable-temperature, solid-state dc and ac magnetic susceptibility studies were carried out on **1**–**4** and revealed the presence of weak ferromagnetic exchange interactions between the metal ions ($J_{Co\text{-}Co}$ = +1.3 and +0.40 cm^{-1} in **1** and **4**, respectively; $J_{Co\text{-}Gd}$ = +0.09 cm^{-1} in **1**). The ac susceptibility studies on **2** revealed nonzero, weak out-of-phase (χ''_M) signals below ~5 K.

Keywords: 3d/4f metal clusters; di-2 pyridyl ketone; magnetism; cobalt; lanthanides; mixed metal Co/Ln clusters

1. Introduction

The synthesis and characterization of new mixed-metal 3d/4f clusters has attracted immense interest over the last few decades, due to their fascinating structural features (high nuclearities, unprecedented metal topologies, aesthetically pleasing architectures, etc.), as well as due to their interesting magnetic properties [1–3]. In particular, 4f ions often favor the formation of heterometallic compounds that possess exceptionally high nuclearities, with representative examples being clusters of $Ni_{64}Gd_{96}$ [4], $Ni_{76}La_{60}$ [5], $Ni_{54}Gd_{54}$ [6], $Cu_{36}Dy_{24}$ [7], $Ni_{10}Gd_{42}$ [8], $Ni_{30}La_{20}$ [9,10], etc. This intriguing ability of 4f ions possibly stems from their strong oxophilicity, which, in combination with their high coordination numbers, results in the formation of hydroxo/oxo species that readily promote the aggregation process. Concerning the magnetic properties of the 3d/4f compounds, the 4f ions bring several advantages, such as their considerable number of unpaired electrons (e.g., Gd^{3+} has seven unpaired e−) and their large single ion anisotropy (e.g., Tb^{3+}, Dy^{3+}, Ho^{3+}, etc.) as a result of

their orbital angular momentum. The above properties make them ideal candidates for the synthesis of heterometallic clusters with single-molecule magnetism behavior (SMMs) [11,12], fulfilling the desirable features for a compound to behave as an SMM, namely (i) high spin ground state (*S*) and (ii) negative axial zero field splitting parameter (*D*). SMMs are discrete metal compounds that exhibit superparamagnetic behavior below a blocking temperature T_B and have been proposed for several technological applications including high-density information storage, molecular spintronics and qubits for quantum computation [11–15].

The study of mixed-metal 3d/4f reaction systems, as a means for the isolation of new SMMs with a high energy barrier for the magnetization reversal, has led to a large variety of such species that now include Mn/4f [16–21], Fe/4f [22–25], Ni/4f [8,26], Cu/4f [27–30] and Co/4f [8,31–33] compounds [1,2]. It is noteworthy that the majority of 3d/4f SMMs are Mn/4f clusters containing some Mn^{III} centers with an S = 2 spin state and a significant uniaxial anisotropy. Some remarkable examples, e.g., a Mn_6Tb_2 [18] and a $Mn_{21}Dy$ [17] cluster, display high energy barriers for the magnetization reversal (U_{eff} = 103 K and 74 K, respectively), which are of comparable magnitude to the family of the most thoroughly studied homometallic carboxylato Mn_{12} SMMs [11]. On the other hand, the reported Co/4f SMMs are significantly less, despite the fact that the combination of the anisotropic $3d^7$ Co^{II} with the 4f ions has a great potential to yield SMMs with high U_{eff} and distinctively different properties from other heterometallic species. A possible explanation for this could be related to synthetic challenges such as the oxidation of the Co^{2+} to the diamagnetic and low spin Co^{3+}, which occurs easily in the presence of a base under ambient conditions.

Many carboxylate and *O* or *N*,*O*-ligands have been used for the synthesis of 3d/4f metal clusters [1–3]; amongst them, di-2-pyridyl ketone ($(py)_2CO$, Scheme 1) is very attractive as its carbonyl group can easily undergo nucleophilic attack, providing a wide range of hemiaketal and *gem*-diol derivatives that are able to link many metal ions, favoring the formation of high nuclearity metal clusters with interesting structural features and magnetic properties [34,35]. Over 200 homo- and heterometallic compounds have now been reported, containing $(py)_2CO$ and its derivatives, thus the absence of such Co/4f clusters is noticeable considering the great development of this research field.

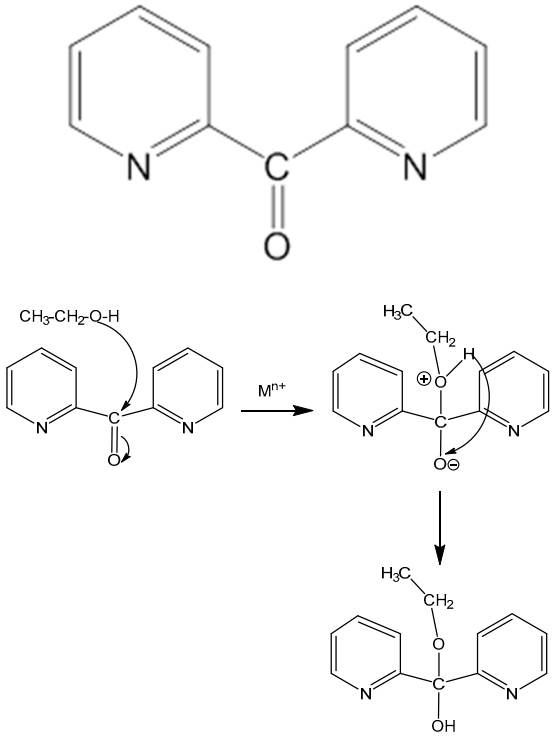

Scheme 1. A schematic representation of $(py)_2CO$ (**top**) and its transformation to $(py)_2C(OEt)(OH)$ (**bottom**).

In 2010, our groups employed $(py)_2CO$ in Ni/4f cluster chemistry and reported a new family of triangular Ni_2Ln compounds with interesting magnetic properties [36,37]. Expanding this research, we herein report the synthesis and characterization of four isostructural triangular Co_2M clusters (M=Tb, Dy, Gd, Y); these compounds are the first examples of Co/4f or Y species bearing $(py)_2CO$ and its derivatives, with the Co_2Dy analogue displaying out-of-phase ac magnetic susceptibility signals at low temperatures, indicative of the slow relaxation of the magnetization.

2. Results and Discussion

2.1. Synthetic Comments

We have developed an intense interest in the synthesis of 3d/4f metal clusters by the employment of various pyridyl oximate- and alkoxide-containing ligands; these research efforts have yielded a variety of new mixed-metal species with interesting structural features and magnetic properties, including Ni_8Dy_8 [38,39], Ni_2Ln_2 [40], Ni_3Ln [26], Ni_2Ln [36,37,40], Mn_4Ln_2 [41], etc. Restricting further discussion to the use of $(py)_2CO$ in this field, we recently reported the first Mn/4f compounds, which belong to a family of cross-shaped Mn_4Ln_2 clusters, where some of them exhibit slow relaxation of magnetization; whereas, in the past, we reported the first Ni/4f compounds with the monoanionic form of $(py)_2CO$. Wishing to expand this work, we recently decided to investigate the previously unexplored reaction system of $Co^{2+}/Ln^{3+}/(py)_2CO$.

The reaction of $Co(ClO_4)_2{\cdot}6H_2O$, $Ln(NO_3)_3{\cdot}6H_2O$ (Ln=Gd, **1**; Dy, **2**; Tb, **3**) or $Y(NO_3)_3{\cdot}6H_2O$ (**4**), $(py)_2CO$ and $CH_3CO_2Na{\cdot}3H_2O$ in EtOH afforded a red solution from which well-shaped red crystals of compounds **1–4** with the general formula $[Co_2M\{(py)_2C(OEt)(O)\}_4(NO_3)(H_2O)]_2[M(NO_3)_5](ClO_4)_2$ were subsequently isolated. The formation of **1–4** is summarized in Equation (1).

$$\begin{gathered} 4\,Co(ClO_4)_2{\cdot}6H_2O + 3M(NO_3)_3{\cdot}6H_2O + 8(py)_2CO + 8NaO_2CMe{\cdot}3H_2O + 8EtOH \xrightarrow{EtOH} \\ \left[Co_2M\left\{(py)_2C(OEt)(O)\right\}_4(NO_3)(H_2O)\right]_2[M(NO_3)_5](ClO_4)_2 + 8MeCO_2H + 2NaNO_3 + 6NaClO_4 + 66H_2O \\ Gd, 1;\ Dy, 2;\ Tb, 3;\ Y, 4 \end{gathered} \quad (1)$$

The nature of the base and the crystallization method are not crucial for the identity of the products and affect only their crystallinity and the reaction yield; we were able to isolate **1–4** (IR evidence) by using other bases, such as NaOMe, NaOEt, $LiOH{\cdot}H_2O$, etc. On the other hand, the ratio of the reactants and the nature of solvent affect the product identity, as by further increasing the excess of $(py)_2CO$, mononuclear Co^{II} compounds are isolated. EtOH is the only solvent that favors the formation of **1–4**, whereas the use of different solvents yields amorphous products that could not be further characterized.

2.2. Description of Structures

A representation of the cationic $[Co_2Gd\{(py)_2C(OEt)(O)\}_4(NO_3)(H_2O)]^{2+}$ that is present in the molecular structure of **1** is shown in Figure 1. A representation of the elipsoid plot for **1** is shown in Figure S1 in the supplementary material. Selected interatomic distances and angles for **1** are listed in Table 1.

Complex **1** crystallizes in the monoclinic space group C 2/c. Its structure consists of two isostructural triangular cationic clusters $[Co_2Gd\{(py)_2C(OEt)(O)\}_4(NO_3)(H_2O)]^{2+}$, which are symmetrically related with a 2-fold crystallographic axis. The positive charge of the cation is balanced by one $[Gd(NO_3)_5]^{2-}$ and two NO_3^- counterions. The cationic cluster is comprised of two Co^{2+} and one Gd^{3+} ions, which are held together by four $(py)_2C(OEt)(O)^-$ ligands. The $\{Co_2GdO_4\}^{3+}$ core of this complex displays an oxo-centered triangular arrangement, in which one μ_3-alkoxo group coming from one $(py)_2C(OEt)(O)^-$ ligand bridges the three metal centres; in addition, three μ_2-O^{2-} ions, from three different $(py)_2C(OEt)(O)^-$ ligands, are located peripherally, bridging the two metal ions in each edge of the triangle. Alternatively, the structural core in **1** can be described as a defective cubane, in which one vertex and three edges are missing. The central μ_3-O^{2-} ion deviates 1.12(2) Å from the plane formed

by the metal ions. The intermetallic distances in **1** are Co1 ... Gd = 3.471 Å, Co2 ... Gd = 3.546 Å and Co1 ... Co2 = 3.192 Å.

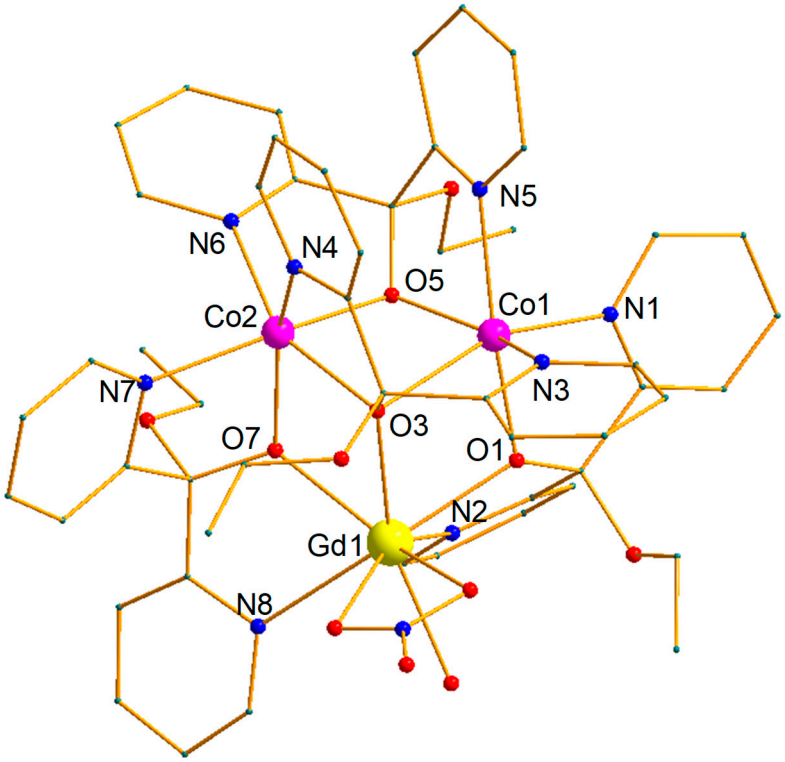

Figure 1. Structure of the cationic cluster **1**. The hydrogen atoms and the counteranions were omitted for clarity.

Table 1. Selected interatomic distances (Å) and angles (degrees) for **1**.

Gd(1)-O(1)	2.252(15)	Co(1)-N(5)	2.220(20)
Gd(1)-O(3)	2.387(15)	Co(2)-O(3)	2.142(13)
Gd(1)-O(7)	2.304(13)	Co(2)-O(5)	2.048(14)
Gd(1)-N(2)	2.582(17)	Co(2)-O(7)	2.046(14)
Gd(1)-N(8)	2.578(19)	Co(2)-N(4)	2.070(16)
Co(1)-O(1)	2.021(15)	Co(2)-N(6)	2.08(2)
Co(1)-O(3)	2.265(15)	Co(2)-N(7)	2.176(19)
Co(1)-O(5)	1.984(16)	Gd(1)-Co(1)	3.471(3)
Co(1)-N(1)	2.083(18)	Gd(1)-Co(2)	3.546(3)
Co(1)-N(3)	2.093(19)	Co(1)-Co(2)	3.192(4)
Co(1)-O(1)-Gd(1)	108.5(6)	Co(2)-O(7)-Gd(1)	109.1(5)
Co(1)-O(3)-Gd(1)	96.5(5)	Co(1)-O(3)-Co(2)	92.8(5)
Co(2)-O(3)-Gd(1)	102.9(6)	Co(1)-O(5)-Co(2)	104.6(7)

The monoanionic $(py)_2C(OEt)(O)^-$ ligands are derived from the nucleophilic attack of one EtOH molecule on the central C atom of the carbonyl group of $(py_2)CO$. The three $(py)_2C(OEt)(O)^-$ ligands adopt a $\eta^1{:}\eta^2{:}\eta^1{:}\mu_2$ coordination mode, with the fourth one being coordinated to the metals in a $\eta^1{:}\eta^3{:}\eta^1{:}\mu_3$ fashion (Scheme 2). The two Co^{II} ions are six-coordinate with their coordination spheres ({O1, O5, O3, N1, N3, N5} for Co1; {O3, O5, O7, N4, N6, N7} for Co2) displaying distorted octahedral geometries. The three O and the three N donor atoms around each Co^{II} ion adopt the facial, fac-topological arrangement; each Co^{II} ion is surrounded by three five-membered chelate rings, formed by three different $(py)_2C(OEt)(O)^-$ ligands. The Co oxidation state was assigned by charge considerations and bond-valence sum (BVS) calculations [42].

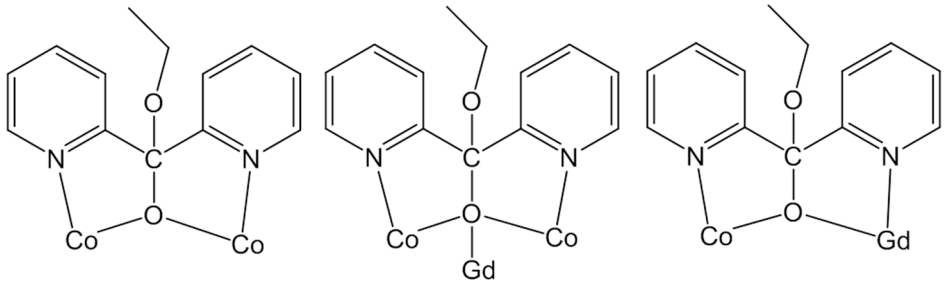

Scheme 2. A schematic representation of the coordination modes of $(py)_2C(OEt)(O)^-$ in **1**.

Gd1 is eight-coordinate and its {O1, O3, O7, O9, O10, O12, N2, N7} coordination sphere is rich in O donor atoms as a consequence of the oxophilic character of the lanthanides. Its coordination environment is formed by two five-membered chelate rings, the central μ_3-O^{2-} ion, one bidentate chelate NO_3^- ion and one terminal H_2O molecule. Gd2 in the $[Gd(NO_3)_5]^{2-}$ ion is 10-coordinated, surrounded by five bidentate chelating nitrate groups. Gd2 lies on a crystallographic 2-fold axis, which passes through the N11 atom of a NO_3^- group.

To deduce the coordination polyhedra defined by the donor atoms around Gd1, a comparison of the experimental structural data with the theoretical data for the most common polyhedral structures with eight vertices was performed by means of the program SHAPE [43,44]; a reliable, high-quality fit was not achieved.

Closer inspection of the crystal structure of **1** reveals the absence of strong H-bonding interactions. This might be a result of the very well-separated neighboring Co_2Gd units. The shortest metal···metal distance between neighboring trinuclear clusters is 10.564 Å (Gd1 … Gd1), while the shortest metal···metal distance between a trinuclear cluster with a neighboring $[Gd(NO_3)_5]^{2-}$ anion is 7.491 Å (Gd1 … Gd2).

Compounds **2**–**4** are isostructural with **1**, as confirmed by a comparison of their unit cell dimensions. The identity, purity and stability of these compounds was also studied by powder X-ray diffraction (pxrd) studies (Figure S2 in the Supplementary Material).

Compound **1** and its structural analogues (**2**–**4**) are the first Co/Ln or Y clusters bearing $(py)_2CO$ and/or its transformed gem-diol or hemiketal derivatives. They also join the very small family of heterometallic 3d/4f/$(py)_2CO$ clusters [26,36,37,41,45,46]; thus, they provide insight into the coordination chemistry of this versatile ligand and unlock the chemical and structural features, which can further lead to the isolation of higher nuclearity heterometallic species.

2.3. Magnetism Studies

Solid-state, variable-temperature dc magnetic susceptibility (χ_M) data were collected on vacuum-dried microcrystalline samples of complexes **1**–**4** in the 2.0–300 K range, and they are shown in Figure 2, top, as $\chi_M T$ vs. T plots. The experimental values for **1**–**4** at 300 K are 16.04, 26.86, 23.09 and 5.5 $cm^3 \cdot K \cdot mol^{-1}$, respectively, being close to the expected ones for one and a half non-interacting Ln^{III} cations (**1**, Gd, S = 7/2, L = 0, $^8S_{7/2}$, g = 2; **2**, Dy, S = 5/2, L = 5, $^6H_{15/2}$, g = 4/3; **3**, Tb, S = 3, L = 3, $^7F_6$, g = 3/2; **4**, Y, S = 0) and two non-interacting high spin Co^{II} cations (S = 3/2, g = 2) of 15.05, 26.1, 21.5 and 3.8 $cm^3 \cdot K \cdot mol^{-1}$, respectively.

The study of the static magnetic properties of highly anisotropic Ln^{III} cations with high-spin Co^{II} ions (S = 3/2) within the same molecule is challenging because both types of paramagnetic centers present spin-orbit contribution due to the strong orbital contribution to the magnetic moment; this yields high anisotropies, which prevent the use of spin-only Hamiltonians for the mathematical interpretation and fitting of the experimental curves [47,48]. Although L is not fully quenched, spin-only Hamiltonians are used to fit the curves for practical reasons, where feasible, in the reported compounds.

For complex **4**, the $\chi_M T$ vs. T curve remains almost constant with the decreasing temperature from 300 to 50 K and then drops to 3.7 $cm^3 \cdot K \cdot mol^{-1}$. This complex contains a diamagnetic Y^{III}, which allows the study of the interaction between the Co(II) ions using the spin Hamiltonian $H = -2J(\hat{S}_{Co1} \cdot \hat{S}_{Co2}) + D\hat{S}_{z2} + \Sigma_i \mu g_{eff} \vec{H} \hat{S}_i$ in the full range of temperature; the exchange interactions between the Co^{II} ions are weak ferromagnetic with J = +0.40 cm^{-1}, D = 9.5 cm^{-1} and g = 2.35.

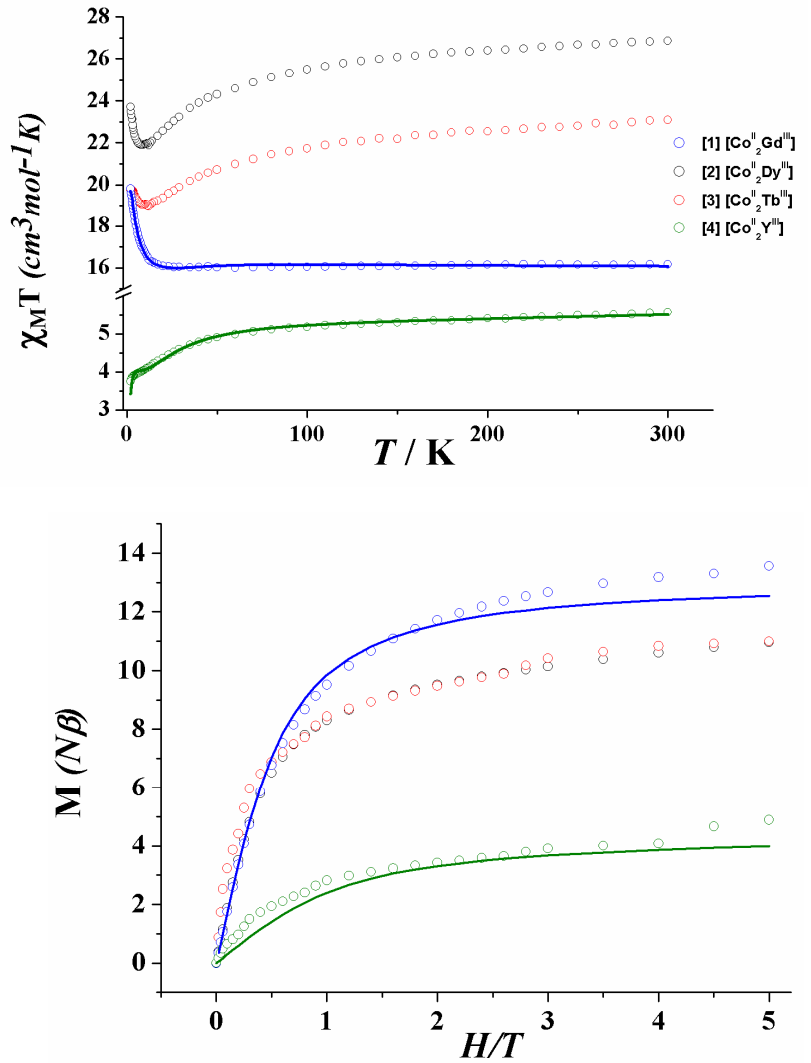

Figure 2. $\chi_M T$ vs. T plots (**top**) and field dependence of the magnetization at 2 K (**bottom**) for **1**–**4**. Solid line represents the best fit for **1** and **4**.

The $\chi_M T$ vs. T curve for **1** remains almost constant until 20 K and then starts to increase, reaching the value of 20.01 $cm^3 \cdot K \cdot mol^{-1}$ at 2 K, which shows an extremely weak ferromagnetic coupling between the metal ions. The fitting of the experimental data to the Hamiltonian equation $H = -2J(\hat{S}_{Co1}\,\hat{S}_{Gd} + \hat{S}_{Co2}\,\hat{S}_{Gd}) - 2J'(\hat{S}_{Co1}\,\hat{S}_{Co2}) + D\hat{S}_z{}^2 + \Sigma_i \mu g_{eff} \vec{H} \hat{S}_i$, in the whole temperature range, provided the coupling values between Co^{II}-Co^{II} ions (J = +1.3 cm^{-1}) and Co^{II}-Gd^{III} ions (J = +0.09 cm^{-1}), respectively, with a mean g value of 2.35. This magnetic coupling is in agreement with previous studies in Co^{II}-Gd^{III} complexes, which always present a ferromagnetic coupling when the Co^{II} is a high spin cation [49,50].

Complexes **2** and **3** exhibit a similar magnetic behavior to that of complex **1**, with a very smooth drop while cooling down due to the depopulation of the Stark sublevels, reaching a minimum (21.88 $cm^3 \cdot K \cdot mol^{-1}$ for **2**; 18.99 $cm^3 \cdot K \cdot mol^{-1}$for **3**) at 12 K.

The field dependence of the magnetization at 2 K for complexes **1**–**4** is shown in Figure 2, bottom. For complexes **1**–**3**, the magnetization increases rapidly below 1 T. For **4**, magnetization presents a value of 3.8 $cm^3 \cdot K \cdot mol^{-1}$, which corresponds to the value of two ferromagnetically coupled Co^{II} cations at 2 K (S = 1/2 for each one). For **1**–**3**, the values of the magnetization at 5 T are 13.5, 10.9 and 10.9 μ_β, respectively.

The study of the dynamic magnetic properties was also performed for all compounds under a zero magnetic field, revealing a clear dependency of the χ_M" on temperature and frequency for complex **2** (Figure S3, Supplementary Material), indicating that **2** might be an extremely weak SMM.

3. Materials and Methods

3.1. Materials, Physical and Spectroscopic Measurements

All manipulations were performed under aerobic conditions using materials (reagent grade) and solvents as received. Elemental analyses (C, H, N) were performed by the University of Patras microanalysis service. IR spectra (4000–400 cm^{-1}) were recorded using a Perkin Elmer 16PC FT-IR spectrometer with samples prepared as KBr pellets. Powder X-ray diffraction data (pxrd) were collected using an Inex Equinox 6000 diffractometer. Solid-state, variable-temperature and variable-field magnetic data were collected on powdered samples using an MPMS5 Quantum Design magnetometer operating at 0.03 T in the 300–2.0 K range for the magnetic susceptibility and at 2.0 K in the 0–5 T range for the magnetization measurements. Diamagnetic corrections were applied to the observed susceptibilities using Pascal's constants. Alternating current (*ac*) magnetic susceptibility experiments were carried out at 1000 Hz.

3.2. Synthesis of $[Co_2Gd\{(py)_2C(OEt)(O)\}_4(NO_3)(H_2O)]_2[Gd(NO_3)_5](ClO_4)_2$ (**1**)

Solid $(py)_2CO$ (0.111 g, 0.60 mmol) and $NaO_2CMe \cdot 3H_2O$ (0.041 g, 0.30 mmol) were added to a pink solution of $Co(ClO_4)_2 \cdot 6H_2O$ (0.110 g, 0.30 mmol) in EtOH (15 mL) under stirring, yielding a red solution. $Gd(NO_3)_3 \cdot 6H_2O$ (0.046 g, 0.10 mmol) was then added and the resulting solution was stirred for 30 min. The red solution was allowed to stand undisturbed in a closed flask. Red prismatic crystals appeared after 2 days, which were collected by filtration, washed with EtOH (2 × 5 mL) and Et_2O (2 × 5 mL) and dried in air. Yield: ~65%. Anal. Calcd (Found) for **1**: C, 38.91 (38.80); H, 3.39 (3.72); N, 10.03 (9.73) %. Selected IR data (KBr, cm^{-1}): 3390 (s,b), 2972 (m), 2928 (w), 2897 (w), 1602 (m), 1568 (w), 1470 (s), 1441 (m), 1384 (s), 1317 (s), 1222 (m), 1090 (s), 1053 (s), 903 (w), 777 (m), 686 (m), 635 (m), 624 (m), 541 (w), 474 (m).

3.3. Synthesis of $[Co_2Dy\{(py)_2C(OEt)(O)\}_4(NO_3)(H_2O)]_2[Dy(NO_3)_5](ClO_4)_2$ (**2**)

This was prepared in the same manner as complex **1** but using $Dy(NO_3)_3 \cdot 6H_2O$ (0.046 g, 0.10 mmol) in place of $Gd(NO_3)_3 \cdot 6H_2O$. After 2 days, red prismatic crystals of **2** appeared, which were collected by filtration, washed with EtOH (2 × 5 mL) and Et_2O (2 × 5 mL) and dried in air. Yield: ~60%. Anal. Calcd (Found) for **2**: C, 38.72 (38.91); H, 3.37 (3.75); N, 9.99 (10.08) %. Selected IR data (KBr, cm^{-1}): 3394 (s,b), 2974 (m), 2930 (w), 2897 (w), 1604 (m), 1570 (w), 1472 (s), 1443 (m), 1384 (s), 1315 (s), 1225 (m), 1090 (s), 1054 (s), 904 (w), 780 (m), 686 (m), 635 (m), 625 (m), 542 (w), 472 (m).

3.4. Synthesis of $[Co_2Tb\{(py)_2C(OEt)(O)\}_4(NO_3)(H_2O)]_2[Tb(NO_3)_5](ClO_4)_2$ (**3**)

This was prepared in the same manner as complex **1** but using $Tb(NO_3)_3 \cdot 6H_2O$ (0.046 g, 0.10 mmol) in place of $Gd(NO_3)_3 \cdot 6H_2O$. After 2 days, red prismatic crystals of **3** appeared, which were collected by filtration, washed with EtOH (2 × 5 mL) and Et_2O (2 × 5 mL) and dried in air. Yield: ~65%. Anal. Calcd (Found) for **3**: C, 38.85 (38.73); H, 3.39 (2.99); N, 10.02 (9.84) %. Selected IR data (KBr, cm^{-1}): v = 3394 (s,b), 2974 (m), 2930 (w), 2896 (w), 1604 (m), 1570 (w), 1472 (s), 1442 (m), 1384 (s), 1316 (s), 1224 (m), 1089 (s), 1054 (s), 904 (w), 780 (m), 686 (m), 636 (m), 626 (m), 542 (w), 474 (m).

3.5. Synthesis of $[Co_2Y\{(py)_2C(OEt)(O)\}_4(NO_3)(H_2O)]_2[Y(NO_3)_5](ClO_4)_2$ (**4**)

This was prepared in the same manner as complex **1** but using $Y(NO_3)_3{\cdot}6H_2O$ (0.038 g, 0.10 mmol) in place of $Gd(NO_3)_3{\cdot}6H_2O$. After 2 days, red prismatic crystals of **4** appeared, which were collected by filtration, washed with EtOH (2 × 5 mL) and Et_2O (2 × 5 mL) and dried in air. Yield: ~65%. Anal. Calcd (Found) for **4**: C, 41.56 (41.47); H, 3.62 (3.53); N, 10.72 (11.09) %. Selected IR data (KBr, cm^{-1}): 3390 (s,b), 2972 (m), 2928 (w), 2897 (w), 1602 (m), 1568 (w), 1470 (s), 1441 (m), 1384 (s), 1317 (s), 1222 (m), 1090 (s), 1053 (s), 903 (w), 777 (m), 686 (m), 635 (m), 624 (m), 541 (w), 474 (m).

Caution! *Although no such behavior was observed during the present work, perchlorate and nitrate salts are potentially explosive; such compounds should be synthesized and used in small quantities, and treated with utmost care at all times.*

3.6. Single-Crystal X-ray Crystallography

Data were collected at the University of Cyprus on an Oxford-Diffraction SuperNova diffractometer, equipped with a CCD area detector and a graphite monochromator utilizing Mo-Kα radiation (λ = 0.71073 Å). Suitable crystals were attached to glass fiber using paratone-N oil and transferred to a goniostat, where they were cooled to 100 K for data collection. Empirical absorption corrections (multi-scan based on symmetry-related measurements) were applied using CrysAlis RED software [51]. The structure was solved by direct methods using SIR92 [52] and refined on F^2 vai the full-matrix least squares method using SHELXL97 [53] and SHELXL-2014/7 [54]. Software packages used are listed as follows: CrysAlisCC for data collection, CrysAlisRED for cell refinement and data reduction [51], WINGX for geometric calculations [55], DIAMOND [56] and MERCURY [57] for molecular graphics. The program SQUEEZE [58], a part of the PLATON package of crystallographic software, was used to remove the contribution of highly disordered solvent molecules. The non-H atoms were treated anisotropically, whereas the H atoms were placed in calculated, ideal positions and refined as riding on their respective C atoms. Unit cell parameters and structure solution and refinement data for **1** are listed in Table S1. An initial search of reciprocal space for **2**–**4** revealed monoclinic cells with dimensions similar to those of **1**; thus, full data collection of their structures was not pursued.

Several crystals of compound **1**, from different preparations and at different periods of time, were carefully tested on the X-rays (using CuKa and MoK radiation) at ambient and low (100 K) temperatures. The diffraction quality of the crystals proved to be moderate and structure determination was eventually carried out by means of the best data set collected. It is important to mention that compound **1** has a unit cell and structure similar to a Ni2Gd analogous compound, as previously reported by us [36,37], though the latter differs mainly in the nature of the 3d metal ion, i.e., it contains Ni^{II} instead of Co^{II}; thus, although the crystallographic data are not of the best quality, the information they provide about the structure is absolutely reliable.

The X-ray crystallographic data for **1** have been deposited with a CCDC reference number CCDC 1906734. They can be obtained free of charge at http://www.ccdc.cam.ac.uk/conts/retrieving.html or from the Cambridge Crystallographic Data Center, 12 Union Road, Cambridge, CB2 1EZ, UK: Fax: +44-1223-336033; or e-mail: deposit@ccdc.cam.ac.uk.

4. Conclusions

Four new mixed-metal Co^{II}_2Ln (Ln = Gd, **1**; Dy, **2**; Tb, **3**) and Co^{II}_2Y (**4**) clusters are described, bearing the anionic hemiaketalic form of di-2-pyridyl ketone as an organic ligand. Compounds **1**–**4** display a triangular metal topology and were synthesized by the reaction of $Co(ClO_4)_2{\cdot}6H_2O$, $M(NO_3)_3{\cdot}6H_2O$, $(py)_2CO$ and $CH_3CO_2Na{\cdot}3H_2O$ in EtOH. They are the first heterometallic Co/4f or Y clusters containing $(py)_2CO$ or its derivatives, and join a very small family of such compounds with this ligand. dc and ac magnetic susceptibility studies revealed the presence of weak ferromagnetic exchange interactions between the metal ions, with **2** exhibiting nonzero, weak out-of-phase (χ″M) signals at temperatures below ~5 K.

$(py)_2CO$ remains a rich wellspring of new metal clusters with interesting structural features and magnetic properties, after many years of intense research efforts that have yielded a massive number of compounds. Further studies on the use of this ligand for the synthesis of new 3d/4f metal clusters are in progress and will be reported in due course.

Supplementary Materials: The following are available online at http://www.mdpi.com/2312-7481/5/2/35/s1: Figure S1. Representation of the elipsoid plot for **1**, Figure S2. Theoretical and experimental pxrd patterns for **1**–**4**, Figure S3: Representation of χ' (black line) and χ'' (red line) for **2**, Figure S4: Linear fit of the ac magnetic suscetibility data for **2** at the frequency of 1000 Hz using the generalized Debye model to extract the slow relaxation parameters, Table S1: Crystallographic data for complex **1**.

Author Contributions: C.G.E. contributed to the synthesis, crystallization and preliminary characterization of all the compounds, and he wrote the relevant draft of the paper. Á.N.F. contributed to the synthesis of **1**–**4**. J.M. performed the magnetic measurements, interpreted the results and wrote the relevant part of the paper. A.T. contributed to the structural characterization of **1**–**4**. S.P.P. contributed to the coordination of the research and interpretation of the results. C.P. contributed to the coordination of the research, collected single crystal X-ray crystallographic data and solved the structure of **1**, and performed refinement in the structure. She also wrote the paper based on the reports of her collaborators.

Funding: J.M. thanks the Ministerio de Economía y Competitividad, Project CTQ2015-63614-P for funding.

Conflicts of Interest: The authors declare no conflict of interest.

References

1. Rosado Piquer, L.; Sañudo, E.C. Heterometallic 3d–4f single-molecule magnets. *Dalton Trans.* **2015**, *44*, 8771–8780. [CrossRef] [PubMed]
2. Liu, K.; Shia, W.; Cheng, P. Toward heterometallic single-molecule magnets: Synthetic strategy, structures and properties of 3d–4f discrete complexes. *Coord. Chem. Rev.* **2015**, *289–290*, 74–122. [CrossRef]
3. Sharples, J.W.; Collison, D. The coordination chemistry and magnetism of some 3d–4f and 4f amino-polyalcohol compounds. *Coord. Chem. Rev.* **2014**, *260*, 1–20. [CrossRef] [PubMed]
4. Chen, W.P.; Liao, P.Q.; Yu, Y.; Zheng, Z.; Chen, X.-M.; Zheng, Y.Z. A Mixed-Ligand Approach for a Gigantic and Hollow Heterometallic Cage {Ni64RE96} for Gas Separation and Magnetic Cooling Applications. *Angew. Chem. Int. Ed.* **2016**, *55*, 9375–9379. [CrossRef] [PubMed]
5. Kong, X.J.; Long, L.-S.; Huang, R.B.; Zheng, L.-S.; Harris, T.D.; Zheng, Z. A four-shell, 136-metal 3d-4f heterometallic cluster approximating a rectangular parallelepiped. *Chem. Commun.* **2009**, 4354–4356. [CrossRef]
6. Kong, X.J.; Ren, Y.P.; Chen, W.X.; Long, L.-S.; Zheng, Z.; Huang, R.-B.; Zheng, L.-S. A Four-Shell, Nesting Doll-like 3d–4f Cluster Containing 108 Metal Ions. *Angew. Chem. Int. Ed.* **2008**, *47*, 2398–2401. [CrossRef]
7. Leng, J.-D.; Liu, J.-L.; Tong, M.-L. Unique nanoscale {CuII36LnIII24} (Ln = Dy and Gd) metallo-rings. *Chem. Commun.* **2012**, *48*, 5286–5288. [CrossRef]
8. Peng, J.-B.; Zhang, Q.-C.; Kong, X.-L.; Zheng, Y.-Z.; Ren, Y.-P.; Long, L.-S.; Huang, R.-B.; Zheng, L.-S.; Zheng, Z. High-Nuclearity 3d−4f Clusters as Enhanced Magnetic Coolers and Molecular Magnets. *J. Am. Chem. Soc.* **2012**, *134*, 3314–3317. [CrossRef]
9. Kong, X.J.; Ren, Y.P.; Long, L.-S.; Zheng, Z.; Nichol, G.; Huang, R.-B.; Zheng, L.-S. Dual Shell-like Magnetic Clusters Containing NiII and LnIII (Ln = La, Pr, and Nd) Ions. *Inorg. Chem.* **2008**, *47*, 2728–2739. [CrossRef]
10. Kong, X.J.; Ren, Y.P.; Long, L.-S.; Zheng, Z.; Huang, R.-B.; Zheng, L.-S. A Keplerate Magnetic Cluster Featuring an Icosidodecahedron of Ni(II) Ions Encapsulating a Dodecahedron of La(III) Ions. *J. Am. Chem. Soc.* **2007**, *129*, 7016–7017. [CrossRef]
11. Bagai, R.; Christou, G. The Drosophila of single-molecule magnetism: $[Mn_{12}O_{12}(O_2CR)_{16}(H_2O)_4]$. *Chem. Soc. Rev.* **2009**, *38*, 1011–1026. [CrossRef]
12. Christou, G.; Gatteschi, D.; Hendrickson, D.N.; Sessoli, R. Single-Molecule Magnets. *MRS Bull.* **2000**, *25*, 66–71. [CrossRef]
13. Wernsdorfer, W.; Bogani, L. Molecular spintronics using single-molecule magnets. *Nat. Mater.* **2008**, *7*, 179–186.
14. Hill, S.; Edwards, R.S.; Aliaga-Alcalde, N.; Christou, G. Quantum Coherence in an Exchange-Coupled Dimer of Single-Molecule Magnets. *Science* **2003**, *302*, 1015–1018. [CrossRef]

15. Tiron, R.; Wernsdorfer, W.; Aliaga-Alcalde, N.; Christou, G. Quantum tunneling in a three-dimensional network of exchange-coupled single-molecule magnets. *Phys. Rev. B* **2003**, *68*, 140407. [CrossRef]
16. Akhtar, M.N.; Lan, Y.; AlDamen, M.A.; Zheng, Y.-Z.; Anson, C.E.; Powell, A.K. Effect of ligand substitution on the SMM properties of three isostructural families of double-cubane Mn_4Ln_2 coordination clusters. *Dalton Trans.* **2018**, *47*, 3485–3495. [CrossRef]
17. Papatriantafyllopoulou, C.; Wernsdorfer, W.; Abboud, K.A.; Christou, G. $Mn_{21}Dy$ Cluster with a Record Magnetization Reversal Barrier for a Mixed 3d/4f Single-Molecule Magnet. *Inorg. Chem.* **2011**, *50*, 421–423. [CrossRef]
18. Holynska, M.; Premuzic, D.; Jeon, I.-R.; Wernsdorfer, W.; Clérac, R.; Dehnen, S. $[Mn^{III}_6O_3Ln_2]$ Single-Molecule Magnets: Increasing the Energy Barrier Above 100 K. *Chem. Eur. J.* **2011**, *17*, 9605–9610. [CrossRef]
19. Stamatatos, T.C.; Teat, S.J.; Wernsdorfer, W.; Christou, G. Enhancing the Quantum Properties of Manganese-Lanthanide Single-Molecule Magnets: Observation of Quantum Tunneling Steps in the Hysteresis Loops of a $\{Mn_{12}Gd\}$ Cluster. *Angew. Chem. Int. Ed.* **2009**, *48*, 521–524. [CrossRef]
20. Mereacre, V.; Ako, A.M.; Clerac, R.; Wernsdorfer, W.; Filoti, G.; Bartolome, J.; Anson, C.E.; Powell, A.K. A Bell-Shaped $Mn_{11}Gd_2$ Single-Molecule Magnet. *J. Am. Chem. Soc.* **2007**, *129*, 9248–9249. [CrossRef]
21. Mereacre, V.; Ako, A.M.; Clerac, R.; Wernsdorfer, W.; Hewitt, I.J.; Anson, C.E.; Powell, A.K. Heterometallic $[Mn_5$-$Ln_4]$ Single-Molecule Magnets with High Anisotropy Barriers. *Chem. Eur. J.* **2008**, *14*, 3577–3584. [CrossRef]
22. Li, H.; Meng, X.; Wang, M.; Wang, Y.-X.; Shi, W.-S.; Cheng, P. A $\{Tb_2Fe_3\}$ Pyramid Single-Molecule Magnet with Ferromagnetic Tb-Fe Interaction. *Chin. J. Chem.* **2019**, *37*, 373–377. [CrossRef]
23. Baniodeh, A.; Liang, Y.; Anson, C.E.; Magnani, N.; Powell, A.K.; Unterreiner, A.N.; Seyfferle, S.; Slota, M.; Dressel, M.; Bogani, L.; et al. Unraveling the Influence of Lanthanide Ions on Intra- and Inter-Molecular Electronic Processes in $Fe_{10}Ln_{10}$ Nano-Toruses. *Adv. Funct. Mater.* **2014**, *24*, 6280–6290. [CrossRef]
24. Badia-Romano, L.; Bartolomé, F.; Bartolomé, J.; Luzón, J.; Prodius, D.; Turta, C.; Mereacre, V.; Wilhelm, F.; Rogalev, A. Field-induced internal Fe and Ln spin reorientation in butterfly $\{Fe_3LnO_2\}$ (Ln = Dy and Gd) single-molecule magnets. *Phys. Rev. B* **2013**, *87*, 184403:1–184403:11. [CrossRef]
25. Schmidt, S.; Prodius, D.; Mereacre, V.; Kostakis, G.E.; Powell, A.K. Unprecedented chemical transformation: Crystallographic evidence for 1,1,2,2-tetrahydroxyethane captured within an Fe_6Dy_3 single molecule magnet. *Chem. Commun.* **2013**, *49*, 1696–1698. [CrossRef]
26. Efthymiou, C.G.; Stamatatos, T.C.; Papatriantafyllopoulou, C.; Tasiopoulos, A.J.; Wernsdorfer, W.; Perlepes, S.P.; Christou, G. Nickel/Lanthanide Single-Molecule Magnets: $\{Ni_3Ln\}$ "Stars" with a Ligand Derived from the Metal-Promoted Reduction of Di-2-pyridyl Ketone under Solvothermal Conditions. *Inorg. Chem.* **2010**, *49*, 9737–9739. [CrossRef]
27. Zhu, Q.; Xiang, S.; Sheng, T.; Yuan, D.; Shen, C.; Tan, C.; Hua, S.; Wu, X. A series of goblet-like heterometallic pentanuclear $[Ln^{III}Cu^{II}_4]$ clusters featuring ferromagnetic coupling and single-molecule magnet behavior. *Chem. Commun.* **2012**, *48*, 10736–10738. [CrossRef]
28. Ghosh, S.; Ida, Y.; Ishida, T.; Ghosh, A. Linker Stoichiometry-Controlled Stepwise Supramolecular Growth of a Flexible Cu_2Tb Single Molecule Magnet from Monomer to Dimer to One-Dimensional Chain. *Cryst. Growth Des.* **2014**, *14*, 2588–2598. [CrossRef]
29. Jose Heras Ojea, M.; Milway, V.A.; Velmurugan, G.A.; Thomas, L.H.; Coles, S.J.; Wilson, C.; Wernsdorfer, W.; Rajaraman, G.; Murrie, M. Enhancement of Tb^{III}–Cu^{II} Single-Molecule Magnet Performance through Structural Modification. *Chem. Eur. J.* **2016**, *22*, 12839–12848. [CrossRef]
30. Baskar, V.; Gopal, K.; Helliwell, M.; Tuna, F.; Wernsdorfer, W.; Winpenny, R.E.P. 3d–4f Clusters with large spin ground states and SMM behavior. *Dalton Trans.* **2010**, *39*, 4747–4750. [CrossRef]
31. Li, X.-L.; Min, F.-Y.; Wang, C.; Lin, S.-Y.; Liu, Z.; Yang, J. Utilizing 3d-4f magnetic interaction to slow the magnetic relaxation of heterometallic complexes. *Inorg. Chem.* **2015**, *54*, 4337–4344. [CrossRef]
32. Chandrasekhar, V.; Pandian, B.M.; Azhakar, R.; Vittal, J.J.; Clérac, R. Linear Trinuclear Mixed-Metal Co^{II}–Gd^{III}–Co^{II} Single-Molecule Magnet: $[L_2Co_2Gd][NO_3]_2CHCl_3$($LH_3$ = (S)P[N(Me)N=CH–C_6H_3-2-OH-3-OMe]$_3$). *Inorg. Chem.* **2007**, *46*, 5140–5142. [CrossRef]
33. Funes, A.V.; Carrella, L.; Rentschler, E.; Alborés, P. $\{Co^{III}_2Dy^{III}_2\}$ single molecule magnet with two resolved thermal activated magnetization relaxation pathways at zero field. *Dalton Trans.* **2014**, *43*, 2361–2364. [CrossRef]

34. Stamatatos, T.C.; Efthymiou, C.G.; Stoumpos, C.C.; Perlepes, S.P. Adventures in the Coordination Chemistry of Di-2-pyridyl Ketone and Related Ligands: From High-Spin Molecules and Single-Molecule Magnets to Coordination Polymers, and from Structural Aesthetics to an Exciting New Reactivity Chemistry of Coordinated Ligands. *Eur. J. Inorg. Chem.* **2009**, *2009*, 3361–3391.
35. Papaefstathiou, G.S.; Perlepes, S.P. Families of Polynuclear Manganese, Cobalt, Nickel and Copper Complexes Stabilized by Various Forms of Di-2-pyridyl Ketone. *Comments Inorg. Chem.* **2002**, *23*, 249–274. [CrossRef]
36. Efthymiou, C.G.; Georgopoulou, A.N.; Papatriantafyllopoulou, C.; Terzis, A.; Raptopoulou, C.P.; Escuer, A.; Perlepes, S.P. Initial employment of di-2-pyridyl ketone as a route to nickel(II)/lanthanide(III) clusters: Triangular Ni_2Ln complexes. *Dalton Trans.* **2010**, *39*, 8603–8605. [CrossRef]
37. Georgopoulou, A.N.; Efthymiou, C.G.; Papatriantafyllopoulou, C.; Psycharis, V.; Raptopoulou, C.P.; Manos, M.; Tasiopoulos, A.; Escuer, A.; Perlepes, S.P. Triangular $Ni^{II}_2Ln^{III}$ and $Ni^{II}_2Y^{III}$ complexes derived from di-2-pyridyl ketone: Synthesis, structures and magnetic properties. *Polyhedron* **2011**, *30*, 2978–2986. [CrossRef]
38. Papatriantafyllopoulou, C.; Stamatatos, T.C.; Efthymiou, C.G.; Cunha-Silva, L.; Almeida Paz, F.; Perlepes, S.P.; Christou, G. A High-Nuclearity 3d/4f Metal Oxime Cluster: An Unusual Ni_8Dy_8 "Core-Shell" Complex from the Use of 2-Pyridinealdoxime. *Inorg. Chem.* **2010**, *49*, 9743–9745. [CrossRef]
39. Polyzou, C.D.; Efthymiou, C.G.; Escuer, A.; Cunha-Silva, L.; Papatriantafyllopoulou, C.; Perlepes, S.P. In search of 3d/4f-metal single-molecule magnets: Nickel(II)/lanthanide(III) coordination clusters. *Pure Appl. Chem.* **2013**, *85*, 315–327. [CrossRef]
40. Papatriantafyllopoulou, C.; Estrader, M.; Efthymiou, C.G.; Dermitzaki, D.; Gkotsis, K.; Terzis, A.; Diaz, C.; Perlepes, S.P. In search for mixed transition metal/lanthanide single-molecule magnets: Synthetic routes to Ni^{II}/Tb^{III} and Ni^{II}/Dy^{III} clusters featuring a 2-pyridyl oximate ligand. *Polyhedron* **2009**, *28*, 1652–1655. [CrossRef]
41. Savva, M.; Skordi, K.; Fournet, A.D.; Thuijs, A.E.; Christou, G.; Perlepes, S.P.; Papatriantafyllopoulou, C.; Tasiopoulos, A.J. Heterometallic $Mn^{III}_4Ln_2$ (Ln = Dy, Gd, Tb) Cross-Shaped Clusters and Their Homometallic $Mn^{III}_4Mn^{II}_2$ Analogues. *Inorg. Chem.* **2017**, *56*, 5657–5668. [CrossRef]
42. Liu, W.; Thorp, H.H. Bond Valence Sum Analysis of Metal-Ligand Bond Lengths in Metalloenzymes and Model Complexes. 2. Refined Distances and Other Enzymes. *Inorg. Chem.* **1993**, *32*, 4102–4105. [CrossRef]
43. Ruiz-Martinez, A.; Casanova, D.; Alvarez, S. Polyhedral Structures with an Odd Number of Vertices: Nine-Coordinate Metal Compounds. *Chem. Eur. J.* **2008**, *14*, 1291–1303. [CrossRef]
44. Llunell, M.; Casanova, D.; Girera, J.; Alemany, P.; Alvarez, S. *SHAPE*, version 2.0; Universitat de Barcelona: Barcelona, Spain, 2010.
45. Georgopoulou, A.N.; Adam, R.; Raptopoulou, C.P.; Psycharis, V.; Ballesteros, R.; Abarca, B.; Boudalis, A.K. Expanding the 3d-4f heterometallic chemistry of the $(py)_2CO$ and pyCOpyCOpy ligands: Structural, magnetic and Mössbauer spectroscopic studies of two Fe^{II}–Gd^{III} complexes. *Dalton Trans.* **2011**, *40*, 8199–8205. [CrossRef]
46. Alexandropoulos, D.I.; Cunha-Silva, L.; Tang, J.; Stamatatos, T.C. Heterometallic Cu/Ln cluster chemistry: Ferromagnetically-coupled $\{Cu_4Ln_2\}$ complexes exhibiting single-molecule magnetism and magnetocaloric properties. *Dalton Trans.* **2018**, *47*, 11934–11941. [CrossRef]
47. Tang, J.; Zhang, P. *Lanthanide Single Molecule Magnets*; Springer: Berlin/Heidelberg, Germany, 2015.
48. Lloret, F.; Julve, M.; Cano, J.; Ruiz-García, R.; Pardo, E. Magnetic properties of six-coordinated high-spin cobalt(II) complexes: Theoretical background and its application. *Inorg. Chim. Acta* **2008**, *361*, 3432–3445. [CrossRef]
49. Xu, Y.; Luo, F.; Zheng, J.-M. Syntheses, Structures, and Magnetic Properties of a Series of Heterotri-, Tetra- and Pentanuclear Ln^{III}–Co^{II} Compounds. *Polymers* **2019**, *11*, 196. [CrossRef]
50. Bartolomé, J.; Filoti, G.; Kuncser, V.; Schinteie, G.; Mereacre, V.; Anson, C.E.; Powell, A.K.; Prodius, D.; Turta, C. Magnetostructural correlations in the tetranuclear series of $\{Fe_3LnO_2\}$ butterfly core clusters:Magnetic and Mössbauer spectroscopic study. *Phys. Rev. B.* **2009**, *80*, 014430:1–014430:16. [CrossRef]
51. Oxford Diffraction. *CrysAlis CCD and CrysAlis RED*, version 1.171.32.15; Oxford Diffraction Ltd.: Oxford, UK, 2008.
52. Altomare, A.; Cascarano, G.; Giaconazzo, C.; Guagliardi, A.; Burla, M.C.; Polidori, G.; Camalli, M. *SIR92: A* program for automatic solution of crystal structures by direct methods. *J. Appl. Crystallogr.* **1994**, *27*, 435–436. [CrossRef]

53. Sheldrick, G.M. *SHELXL97*; University of Göttingen: Göttingen, Germany, 1997.
54. Sheldrick, G.M. *SHELXL-2014/7*; Program for Refinement of Crystal Structures, University of Göttingen: Göttingen, Germany, 2014.
55. Farrugia, L.J. WinGX suite for small-molecule single-crystal crystallography. *J. Appl. Crystallogr.* **1999**, *32*, 837–838. [CrossRef]
56. Brandenburg, K. *DIAMOND*; Version 3.1d; Crystal Impact GbR: Bonn, Germany, 2006.
57. Macrae, C.F.; Edgington, P.R.; McCabe, P.; Pidcock, E.; Shields, G.P.; Taylor, R.; Towler, M.; Van de Streek, J. Mercury: Visualization and analysis of crystal structures. *J. Appl. Crystallogr.* **2006**, *39*, 453–457. [CrossRef]
58. Van der Sluis, P.; Spek, A.L. BYPASS: An Effective Method for the Refinement of Crystal Structures Containing Disordered Solvent Regions. *Acta Crystallogr. Sect. A Found Crystallogr.* **1990**, *A46*, 194–201. [CrossRef]